



HAL
open science

Sunlab: a Functional-Structural Model for Genotypic and Phenotypic Characterization of the Sunflower Crop

Fenni Kang, Paul-Henry Cournede, Jeremie Lecoer, Véronique Letort

► To cite this version:

Fenni Kang, Paul-Henry Cournede, Jeremie Lecoer, Véronique Letort. Sunlab: a Functional-Structural Model for Genotypic and Phenotypic Characterization of the Sunflower Crop. *Ecological Modelling*, 2014, 290, pp.21-33. 10.1016/j.ecolmodel.2014.02.006 . hal-01272125

HAL Id: hal-01272125

<https://hal.science/hal-01272125>

Submitted on 10 Feb 2016

HAL is a multi-disciplinary open access archive for the deposit and dissemination of scientific research documents, whether they are published or not. The documents may come from teaching and research institutions in France or abroad, or from public or private research centers.

L'archive ouverte pluridisciplinaire **HAL**, est destinée au dépôt et à la diffusion de documents scientifiques de niveau recherche, publiés ou non, émanant des établissements d'enseignement et de recherche français ou étrangers, des laboratoires publics ou privés.

1 Sunlab: a Functional-Structural Model for Genotypic
2 and Phenotypic Characterization of the Sunflower Crop

3 Fenni Kang^a, Paul-Henry Courneade^a, Jeremie Lecoeur^b, Veronique
4 Letort^{a,*}

5 ^aLaboratory MAS, Ecole Centrale Paris, Grande Voie des Vignes, F-92 295
6 Chatenay-Malabry, France

7 ^bMontpellier SupAgro, 2, Place Pierre Viala, 34060 Montpellier Cedex 2

8 **Abstract**

A new functional-structural model SUNLAB for the crop sunflower (*Helianthus annuus* L.) was developed. It is dedicated to simulate the sunflower organogenesis, morphogenesis, biomass accumulation and biomass partitioning to organs. It is adapted to model phenotypic responses of different genotypic variants to diverse environmental factors including temperature stress and water deficit. A sensitivity analysis was conducted to quantify the relative parameter influences on the main trait of interest, the grain yield. The model was calibrated for four genotypes on two experimental datasets collected on plants grown under standard non-limiting conditions and moderate water stress. Its predictive ability was then tested on an additional dataset. The four considered genotypes - “Albena”, “Melody”, “Heliasol” and “Prodisol” - are the products of more than 30 years of breeding effort. Comparing the values found for the four parameter sets associated to each variant, allows to identify genotype-specific parameters. The model also provides a novel way of investigating genotype performances under different environmental conditions. These promising results are a first step towards

*Corresponding author, Tel.:(33)1 41 13 17 65
Preprint submitted to Ecological Modelling
Email addresses: fennikang@hotmail.com (Fenni Kang),
veronique.letort@ecp.fr (Veronique Letort)

January 4, 2014

the potential use of the model as a support tool to design sunflower ideotypes adapted to the current worldwide ecological and economical challenges and to assist the breeding procedure.

9 *Keywords:* SUNLAB, SUNFLO, GREENLAB, Sunflower model

10 **1. Introduction**

11 As one of the major oilseed crops worldwide, sunflower production has
12 to face the growing social demand in a context of strong ecological and eco-
13 nomical constraints: growers are confronted to the challenge of increasing
14 sunflower productivity under changing climatic conditions while maintaining
15 low input levels and reduced costs. A partial response to this challenge could
16 be found by breeding new genotypes or by identifying the best genotype,
17 among a set of existing ones, for a given location and for given management
18 practices; see for instance Allinne et al. (2009).

19 Assessments of genotype performances for *in situ* experimental trials ham-
20 per the breeding process by temporal, logistic and economical difficulties.
21 Indeed, genotypes perform differently depending on the environmental con-
22 ditions (soil, climate, etc.) and the management practices (sowing date,
23 nitrogen inputs, irrigation, etc.). Therefore a large number of trials are
24 needed to explore a sufficiently diverse set of genotypes x environment x
25 management (GxExM) combinations in order to characterize these complex
26 interactions. An emerging approach to overcome these difficulties relies on
27 the use of models represented as a set of biophysical functions that deter-
28 mine the plant phenotype in response to environmental inputs. Models can
29 help in breeding strategies and management by dissecting physiological traits

30 into their constitutive components and thus allow shifting from highly inte-
31 grated traits to more gene-related traits that should reveal more stable under
32 varying environmental conditions (Yin et al., 2004; Hammer et al., 2006).

33 Consequently, an important question to examine is how to design models
34 that can be used in that context. The models should simulate the phenotypic
35 traits of interest (e.g. yield) with good robustness and predictive capacity.
36 The models should also present a trade-off between mechanistic aspect and
37 complexity: Chapman et al. (2003) state that, for such use, a growth model
38 should include ‘principles of response and feedbacks’ to ‘handle perturbations
39 to any process and self-correct, as do plants under hormonal control when
40 growing in the field’ and to ‘express complex behavior even given simple op-
41 erational rules at a functional crop physiological level’. Casadebaig et al.
42 (2011) discuss that question in the case of their model SUNFLO (Lecoeur
43 et al., 2011). SUNFLO is a biophysical plant model that describes organo-
44 genesis, morphogenesis, and metabolism of sunflower (*Helianthus annuus L.*).
45 It has shown good performances to identify, quantify, and model phenotypic
46 variability of sunflower at the individual level in response to the main abi-
47 otic stresses occurring at field level but also in the expression of genotypic
48 variability (Casadebaig et al., 2011). The authors mixed mechanistic and sta-
49 tistical approaches to deal with highly integrative variables such as harvest
50 index (HI). This HI factor is determined by a simple statistical relation-
51 ship dependent on covariables previously simulated by the mechanistic part
52 of the crop model throughout the growing season. Although this statistical
53 solution and the large datasets used for its parameterization conferred good
54 robustness to the prediction of HI and thereby crop harvest, biomass parti-

55 tioning to other plant organs and trophic competition between organs were
56 not taken into account. Fenni: Here, in last review, the third reviewer posed
57 a question “ The idea of formalizing trophic competition between organs (p 4
58 l 27-33) is at the core of this new model. You write that such a formalization
59 should help representing feedback effects of biomass partitioning on “other
60 processes” (p 4 l 13-15). What do you mean?”, I simply deleted the sentence
61 that saying “feedback effects of biomass partitioning on other processes can-
62 not be taken into account”, but I still tried to mention it in the discussion
63 saying “The plants are considered only at the minimal level of organ com-
64 partments. PBM model ignores plant architecture and its plasticity. The
65 lack of individual organ’s simulation can influence the simulation of plant
66 functioning. For example, PBMs models normally use the relative values of
67 the sink strength of organs to simulate biomass partitioning. These sink val-
68 ues are assessed directly from experiments and the sources and sinks have no
69 significant direct interaction in these models (de Reffye et al., 2008). How-
70 ever, the lack of trophic competition simulation may hinder the simulation of
71 feedback effects of biomass partitioning on other processes. As Pallas et al.
72 (2008) state, trophic competition influenced the organogenesis of grapevine
73 in their research”. That paragraph had been deleted by you in last revision.
74 Do you think we should still mention somewhere this idea “mechanistic sink-
75 source solver helps the simulation of biomass partitioning, and also the future
76 possibility of simulating feedback effects”?. I added one sentence in the dis-
77 cussion to add about considering feedback effects:”Introducing a mechanism
78 of trophic competition at organ level in a PBM, as done in this study, opens
79 the possibility to model feedbacks effects of biomass partitioning on other

80 processes such as photosynthesis or organogenesis (Mathieu et al., 2009).
81 ”“. Do you agree? Moreover, it was shown in Lecoecur et al. (2011) that
82 *HI* is the parameter that contributes the most (14.3%) to the coefficient of
83 variation of the potential grain yield. It was also shown that when ranking
84 the processes in terms of their impact on yield variability, the first one was
85 biomass allocation (before light interception according to plant architecture,
86 plant phenology and photosynthesis). Therefore, Lecoecur et al. (2011) sug-
87 gested that a better formalisation of the trophic competition between organs
88 could be a way to improve our understanding of genotypic variation for the
89 harvest index Fenni: here the third reviewer posed another question last
90 time “ Please elaborate and give appropriate references to clarify the idea of
91 formalizing trophic competition (direct formalization? It could also be indi-
92 rect) and to construct a sound argument (e.g. which outlines to satisfy the
93 need of feedback effects of biomass partitioning).” I actually didn’t answer
94 his question about direct formalization or indirectIn fact I don’t understand
95 the reviewer’s question; what do you think he means by ”‘direct or indi-
96 rect formalization’”? In order to take up this challenge, a new sunflower
97 model, named SUNLAB, was derived from SUNFLO. The representation
98 of plant topological development and allocation process at individual organ
99 scale were inspired by the functional-structural plant model GREENLAB,
100 which has been designed as a “source-sink solver” (Christophe et al., 2008)
101 and which is accompanied with the appropriate mathematical tools for its
102 identification (Cournede et al., 2011). SUNLAB thus inherits from GREEN-
103 LAB the flexible rules of sink competition for biomass partitioning at organ
104 scale Fenni:the deleted phrases “(organ type includes blade, petiole, intern-

105 ode and capitulum; a leaf consists of a blade and a petiole; for the modeling
106 of trophic competition, blade and petiole are considered as two organ types)”
107 were actually trying to answer the second reviewer’s question in the previous
108 review “ you are using the word “blade” to designate the leaves all over the
109 manuscript. This is somewhere confusing. The manuscript would benefit to
110 clarify this”. Maybe somewhere a small explanation of blade could be added
111 if it is deleted here Yes, I had taken care of that and I had added it in the MM
112 part, in *plantstructure* paragraph as ” ‘ The different organ types, denoted as
113 o, include leaves (decomposed into blades and petioles),” ’ Do you think that
114 it will be ok ?, together with the more detailed representation of ecophysio-
115 logical processes and environmental stress effects on biomass production and
116 yield from SUNFLO.

117 This paper presents in detail the mechanisms of SUNLAB and the pa-
118 rameter estimation procedure based on field experimental data. A sensitivity
119 analysis is performed on the model parameters, using the Sobol method, to
120 investigate the relative contribution of each parameter and their interac-
121 tions to the model output uncertainty. The output that we consider is the
122 main trait of interest in most breeding procedures, that is the final grain
123 yield. The potentials of SUNLAB for genotypic characterization are illus-
124 trated by comparing the parameters obtained after the estimation process
125 for four genotypes, namely “Albena”, “Heliasol”, “Melody” and “Prodisol”.
126 The performances of SUNLAB to reproduce phenotypic variability coming
127 either from genotypic or from environmental influences are tested against
128 experimental datasets used for parameterization. An additional dataset is
129 then used for model evaluation. An interesting and uncommon output of

130 SUNLAB is the simulation of specific leaf area (SLA, also known as leaf spe-
131 cific surface area, $cm^2.g^{-1}$), *i.e.* the ratio of leaf area to dry leaf mass. It is
132 an influent input variable often associated with large uncertainty ranges in
133 most dynamic crop growth models (Rawson et al., 1987).

134 **2. Materials and methods**

135 *2.1. Modeling: SUNLAB modules*

136 SUNLAB consists of five modules: phenology, water budget, organogen-
137 esis and morphogenesis, biomass accumulation, and biomass partitioning.
138 Phenology, water budget, and biomass accumulation modules are directly
139 inherited from the SUNFLO model. The organogenesis and morphogenesis
140 module is modified from the corresponding SUNFLO module by defining for
141 each organ the dates, expressed in thermal time, of initialization, termination
142 of its growth, and organ expansion. The biomass partitioning module is an
143 entirely new module. We describe here equations of these modules, briefly
144 for those inherited from SUNFLO - we refer to Casadebaig et al. (2011) and
145 Lecoeur et al. (2011) for an exhaustive description - and in detail for the
146 new contributions. Model parameters that are mentioned in the following
147 equations will be summarized in section 2.3.

148 *2.1.1. Phenology*

149 Plant phenology is driven by thermal time. Cumulative thermal time on
150 day d since emergence, $CTT(d)$ ($^{\circ}C\ days$), is calculated in equation (1) as
151 the sum of the daily mean air temperature $T_m(d)$ ($^{\circ}C$) above a base tem-
152 perature T_b of $4.8\ ^{\circ}C$, common to all sunflower genotypes. Four key phe-
153 nological stages, expressed as genotype-dependent thermal dates ($^{\circ}C\ days$),

154 are defined: flower bud appearance $E1$, beginning of flowering $F1$, begin-
 155 ning of grain filling $M0$ (early maturation) and physiological maturity $M3$
 156 (Lecoeur et al., 2011). Crop development can be accelerated by water stress,
 157 that causes overheating of the plant through the reduction of transpiration.
 158 This is modeled by using a multiplicative effect of water stress at day d ,
 159 $FHTR(d)$ (the effect of water on transpiration), on thermal time accumula-
 160 tion $CTT(d)$:

$$T_{eff}(d) = \max(0, (T_m(d) - T_b))$$

$$CTT(d) = \sum_{k=1}^d T_{eff}(k) \times [1 + 0.1 \times (1 - FHTR(k))] \quad (1)$$

161 where $T_{eff}(k)$ is the effective thermal time at day k . $FHTR(d)$ is calculated
 162 as a function of the fraction of transpirable soil water at day d , $FTSW(d)$
 163 (detailed in 2.1.2), divided by a genotypic parameter RT of sensitivity to
 164 water deficiency (Casadebaig et al. (2011)).

165 2.1.2. Water budget

166 In SUNLAB, the water cycle of sunflower is modeled considering the plant
 167 processes (root water absorption and transpiration), in combination with its
 168 direct environment: precipitation, irrigation, soil evaporation (see Fig. 1a).
 169 Evaporation and plant transpiration decrease the available amount of water
 170 in soil, while irrigation and precipitation refill it.

171 [Figure 1 about here.]

172 The index for the assessment of drought level $FTSW(d)$ at day d depends
 173 on the simulation of the above mentioned processes (Lecoeur et al., 2011).
 174 It takes values from 0 (no water stress) to 1 (severe water stress) and it is

175 used to define three indices to tune three plant functioning processes: leaf
 176 expansion $FHLE$, radiation use efficiency $FHRUE$ and plant transpiration
 177 $FHTR$. The critical thresholds RT and RO are genotype-dependent pa-
 178 rameters varying in $[0, 1]$ that characterize the plant drought tolerance (RT ,
 179 drought tolerance of leaf expansion; RO , drought tolerance of radiation use
 180 efficiency and transpiration). For instance, $FHRUE$ is calculated as:

$$FHRUE(d) = \begin{cases} FTSW(d)/RT & \text{for } FTSW(d) < RT \\ 1 & \text{for } FTSW(d) \geq RT \end{cases} \quad (2)$$

181 Its effect on radiation use efficiency $RUE(d)$ ($g.MJ^{-1}$) is defined as:

$$RUE(d) = RUE_p(d) \times \min\left(1, \frac{FTSW(d)}{RT}\right) \times FT(d) \times PHS \quad (3)$$

182 where $RUE_p(d)$ ($g.MJ^{-1}$) is the crop potential (maximal) radiation use ef-
 183 ficiency, $FT(d)$ is the thermal stress on day d , a function of daily mean
 184 temperature (Lecoeur et al., 2011) and PHS is a genotypic parameter giving
 185 the ratio of the genotype photosynthesis capacity to that of the reference
 186 genotype “Melody”. The potential radiation use efficiency is thus weakened
 187 by the environmental thermal stress factor $FT(d)$ and the drought stress
 188 factor $FHRUE(d)$.

189 2.1.3. Organogenesis and morphogenesis

190 *Ecophysiological functions.* The number of blades $N(d)$ on day d increases
 191 linearly with cumulative thermal time $CTT(d)$:

$$N(d) = R \times CTT(d) + 1 \quad (4)$$

192 where R (leaves/ (°C days)) is the rate of leaf production. Leaf senescence
 193 occurs during the period of grain filling between M0 and M3. Consequently

194 the number of senescent leaves $NS(d)$ is considered to increase in proportion
 195 to the time elapsed since $M0$ (Sinclair and de Wit, 1975; Nooden et al., 1997)
 196 as:

$$NS(d) = N_{total} \times \frac{M3 - CTT(d)}{M3 - M0} \quad (5)$$

197 where N_{total} is a genotypic parameter equal to the maximal number of leaves.
 198 Since, in sunflower, leaf area distribution along the stem shows a bell shape,
 199 total leaf area $A(d)$ (cm^2) per plant is calculated with a logistic equation:

$$A(d) = \frac{A1}{1 + e^{4 \times A3 \times (A2 - N(d)) / A1}} \quad (6)$$

200 where $A1$ (cm^2) is the maximal leaf area, $A2$ and $A3$ (cm^2) are respectively
 201 the rank and the area of the largest leaf of the plant. The calculation of
 202 senescent leaf area $AS(d)$ (cm^2) is determined by a similar logistic equation
 203 but replacing $N(d)$ by $NS(d)$. The photosynthetically active leaf area $AA(d)$
 204 (cm^2) is estimated as the difference between total leaf area $A(d)$ and senescent
 205 leaf area $AS(d)$. Leaf growth and senescence are affected by water stress and
 206 temperature stress coefficients as described in Casadebaig et al. (2011).

$$AA(d) = \frac{A1}{1 + e^{4 \times A3 \times (A2 - N(d)) / A1}} - \frac{A1}{1 + e^{4 \times A3 \times (A2 - NS(d)) / A1}} \quad (7)$$

207 *Plant structure.* The different organ types, denoted as o , include leaves (de-
 208 composed into blades and petioles), internodes and capitulum. For each
 209 individual organ o at rank i (i takes its values from 0 to the total amount of
 210 individual organs of type o), its emergence thermal time $initTT(o, i)$, senes-
 211 cence thermal time $seneTT(o, i)$, and growth expansion duration in thermal
 212 time $epdTT(o, i)$ are defined. The thermal time of blade emergence and

213 senescence are calculated through inversion of equations 4 and 5:

$$\begin{aligned}
 \text{initTT}(\text{blade}, i) &= (i - 1)/R \\
 \text{seneTT}(\text{blade}, i) &= M3 - \frac{i \times (M3 - M1)}{N_{total}}
 \end{aligned}
 \tag{8}$$

214 For the calculation of blade expansion duration $\text{epdTT}(\text{blade}, i)$, three pa-
 215 rameters initTTAdjust ($^{\circ}\text{C days}$), epdTTA ($^{\circ}\text{C days}$), epdTtB ($^{\circ}\text{C days}$)
 216 are added to the module to calculate $\text{epdTT}(\text{blade}, i)$ based on the blade
 217 emergence and senescence thermal times:

$$\begin{aligned}
 \text{epdTT}(\text{blade}, i) &= \text{seneTT}(\text{blade}, i) - (\text{epdTtB} - \text{epdTtA} \times i) \\
 &\quad - (\text{initTT}(\text{blade}, i) - \text{initTTAdjust})
 \end{aligned}
 \tag{9}$$

218 Since leaf emergence was recorded when lengths of their central vein are big-
 219 ger than 4cm (Lecoeur et al., 2011), the leaf has already received a small
 220 amount of biomass at the recorded thermal time $\text{initTT}(\text{blade}, i)$. There-
 221 fore, thermal time of blade growth initialization is calculated by subtracting
 222 initTTAdjust to the emergence thermal time $\text{initTT}(\text{blade}, i)$. The thermal
 223 times of end of blade expansion linearly vary with their ranks and depend
 224 on two parameters, epdTtA and epdTtB .

225 The petiole at rank i shares the same initial, senescence and expansion
 226 thermal times as the blade i belonging to the same metamer. The internode
 227 i has also the same emergence thermal time as the blade i while its expan-
 228 sion duration $\text{epdTT}(\text{internode}, i)$ is driven by a parameter internodeEpdTT
 229 that is common to all internodes. Capitulum initialization thermal time
 230 corresponds to $M0$. Its expansion duration is defined by the parameter
 231 capitulumEpdTT . These additional parameters to the module are estimated
 232 as described in 2.3.

233 With all the information of emergence and senescence thermal times of ev-
234 ery organ, a general sunflower structure can be constructed. Their expansion
235 durations are important variables for the calculation of biomass distribution
236 to organs as presented in 2.1.5.

237 2.1.4. Biomass accumulation

238 Daily increase in above-ground dry matter $DM(d)$ ($g.m^{-2}$) is calculated
239 from Monteith's equation (1977) linking dry matter production to incom-
240 ing photosynthetically active radiation through two radiation efficiencies as
241 follows:

$$DM(d) = RUE(d) \times RIE(d) \times PAR_0(d) \quad (10)$$

242 where $PAR_0(d)$ ($MJ.m^{-2}$) is the daily incident photosynthetically active
243 radiation. $RUE(d)$ ($g.MJ^{-1}$) is daily radiation use efficiency and $RIE(d)$
244 is daily radiation interception efficiency, estimated from Beer's law. The
245 total above-ground biomass $CDM(d)$ ($g.m^{-2}$) is the cumulated daily biomass
246 production from emergence:

$$CDM(d) = \sum_{k=1}^d DM(k) \quad (11)$$

247 2.1.5. Biomass partitioning

248 As in GREENLAB, the biomass produced by leaves is distributed to
249 all organs proportionally to their respective demands. Indeed, it has been
250 observed for several crops that the final balance of the source and sink rela-
251 tionships in the end is similar to the action of a common pool of biomass (e.g.
252 Heuvelink (1995) for tomato): this simplification enables skipping the details
253 of the transport resistance system and other complex features of branching

254 systems (Christophe et al., 2008). The biomass is dynamically distributed to
 255 every “sink” organ, including blades, petioles, internodes and the capitulum,
 256 regardless of their position within the plant structure. Blades are “sources”
 257 whose photosynthetic production fills the pool biomass. The calculation of
 258 the daily incremental mass of each organ is done through three steps.

259 *First step: Definition of individual organ sink.* Biomass is partitioned to
 260 organs according to their number, age and relative sink strength. The relative
 261 sink strength of organs of given type o is denoted as $SR(o)$, which is a
 262 dimensionless variable indicating the ability of different kinds of organs in
 263 competing for biomass. The relative sink strength of all blades is set to 1 as
 264 a reference value, i.e. $SR(blade) = 1$ (Kang et al., 2008). The growth rate
 265 of an individual organ can vary through its expansion period. This change
 266 is modeled by a normalized discrete Beta density function in GREENLAB
 267 model (Kang et al., 2008) and in this model. Among any empirical functions
 268 that could be suitable, the Beta function is recommended by Yin et al. (2003)
 269 as it presents several advantages: at initial and final times, its values are zero,
 270 it has a high flexibility and can describe asymmetric growth trajectories and
 271 it has stable parameters for statistical estimation. Therefore, the actual sink
 272 strength of an organ $SAP(d, o, i)$ (e.g. the actual sink strength an organ of
 273 type $o = blade$, at rank $i = 2$, on day d $SAP(d, blade, 2)$) can be expressed
 274 as:

$$\begin{aligned}
 SAP(d, o, i) &= \left(1 - \frac{CTT(d) + initTT(o, i)}{epdTT(o, i)}\right)^{sinkB(o)-1} \\
 &\times \left(\frac{CTT(d) - initTT(o, i)}{epdTT(o, i)}\right)^{sinkA(o)-1} \times \frac{SR(o)}{M(sinkA(o), sinkB(o))}
 \end{aligned} \tag{12}$$

275 where $M(A, B)$ is a normalization factor defined as:

$$M(A, B) = \left(\frac{A-1}{A+B-2}\right)^{A-1} \times \left(1 - \frac{A-1}{A+B-2}\right)^{B-1} \quad (13)$$

276 Two organ-type-specific parameters $sinkA(o)$ and $sinkB(o)$ control the
 277 function shape, as illustrated in the result section Fig.4. Thus, the sink
 278 activity of an organ o at rank i starts from $initTT(o, i)$ and lasts during the
 279 organ's expansion duration $epdTT(o, i)$.

280 *Second step: Total demand.* The plant total demand $sumSink(d)$ is com-
 281 puted as the scalar product of the number of existing organs by their sink
 282 strength $SAP(d, o, i)$:

$$sumSink(d) = \sum_t \sum_i SAP(d, o, i) \quad (14)$$

283 *Third step: biomass partitioning to organs.* The total dry biomass $CDM(d)$
 284 that is produced at day d is allocated to every individual organs propor-
 285 tionally the ratio of their sink strength $SAP(d, o, i)$ to the total plant de-
 286 mand $sumSink(d)$. For example the biomass allocated to an individual blade
 287 $indMS(d, blade, i)$ ($g.m^{-2}$) of blade ranking i is:

$$indMS(d, blade, i) = \frac{CDM(d) \times SAP(d, blade, i)}{sumSink(d)} \quad (15)$$

288 Total blade biomass $organMS(d, blade)$ ($g.m^{-2}$) at time d is the sum of all
 289 individual blade biomass:

$$organMS(d, blade) = \sum_i indMS(d, blade, i) \quad (16)$$

290 Similarly, individual and total petiole biomass ($indMS(d, petiole, i)$ and $organMS(d, petiole)$,
 291 $g.m^{-2}$) are simulated, as well as individual and total internode biomass
 292 ($indMS(d, internode, i)$ and $organMS(d, internode)$, $g.m^{-2}$), and capitu-
 293 lum biomass ($indMS(d, capitulum, i)$ $organMS(d, capitulum)$, $g.m^{-2}$).

294 *2.2. Field experiments and measurements*

295 Experiments and measurements for designing and constructing modules
296 which are directly inherited from SUNFLO are not presented in this paper, as
297 they are described in detail in Lecoeur et al. (2011). Data used for SUNLAB
298 parameters estimation, simulation and application include three datasets, re-
299 spectively entitled as “2001”, “2002a” and “2002b”. They all come from field
300 experiments conducted in 2001 and 2002 at SupAgro experimental station at
301 Lavalette (43° 36’N, 3° 53’ E, altitude 50 *m*) on a sandy loam soil for four
302 genotypes “Albena”, “Heliasol”, “Melody” and “Prodisol”. In “2001”, Sun-
303 flowers were sown on 5 May 2001 at a density of about 6 plants m^{-2} and a
304 row spacing of 0.6 m, in a randomized complete block design with four repli-
305 cations. Plots measured 5.5. \times 13.0 *m*. In the other two datasets, experiments
306 were conducted with the same plant arrangement. But sunflowers were sown
307 on 15 May 2002 and plots measured 8.0 \times 8.0 *m*. During the experiment,
308 meteorological data such as temperatures and radiation were recorded. The
309 total amount of water available for the plant was calculated as the differ-
310 ence between soil water content at field capacity estimated at the beginning
311 of the experiment and soil water content at 10% of maximal stomatal con-
312 ductance. The fraction of transpirable soil water (*FTSW*) remaining in the
313 soil at a given date was calculated as the ratio of actual plant-available soil
314 water content to the total plant-available soil water content (Lebon et al.,
315 2006). Organogenesis was described based on the phenomenological stages
316 that were recorded every 2-3 days (Lecoeur et al., 2011). Once a week, six
317 plants per genotype were harvested. Individual leaf areas were estimated
318 from blade lengths and widths. All the above-ground organs (blades, peti-

319 oles, stem, capitulum and seeds) were collected and then oven-dried at 80°C
320 for 48 h. The dry weights of these organs were measured by compartments.
321 Daily radiation interception efficiency $RIE(d)$ and daily radiation use ef-
322 ficiency $RUE(d)$ were respectively calculated and estimated based on field
323 measurements as in (Lecoeur et al., 2011). In all experiments, the crop was
324 regularly irrigated and fertilized to avoid severe water deficits and mineral
325 deficiency. But in practice, the three experiments showed different water
326 deficit conditions. The index $FTSW$ of the three experiments, which can
327 represent the water stress level, is illustrated (Fig.2). Since the experiment
328 measurements were carried out every a few days, an interpolation on exper-
329 imental data was drawn to make the contrast clearer. Datasets “2001” and
330 “2002a” correspond to contrasted environmental conditions and are used to
331 calibrate SUNLAB model while “2002b” is used for model evaluation.

332 [Figure 2 about here.]

333 2.3. Parameter analysis

334 Four genotypes “Albena”, “Melody”, “Heliasol” and “Prodisol” are con-
335 sidered in this paper. These genotypes have been characterized by a large
336 study of genetic improvement of sunflower over the last 30 years, and they
337 are four of those most widely grown varieties in France from 1960 to 2000
338 (Vear et al., 2003). SUNLAB parameters can be decomposed in two subsets.
339 One subset contains the parameters inherited from SUNFLO which keep the
340 same values in SUNLAB (Table 1).

341 [Table 1 about here.]

342 The other subset contains 17 additional parameters, that are introduced in
343 SUNLAB, as was presented in section 2.1. They include 12 parameters that
344 drive the sink competition (SR , $sinkA$, $sinkB$ for four types of organs) and 5
345 parameters, that are used to adjust or define initial and final organ expansion
346 thermal times: $initTTAdjust$ ($^{\circ}C\ days$), $epdTTA$ ($^{\circ}C\ days$), $epdTTB$ ($^{\circ}C$
347 $days$), $internodeEpdTT$ ($^{\circ}C\ days$), and $capitulumEpdTT$ ($^{\circ}C\ days$). Note
348 that the sink strength of blades $SR(blade)$ is set to 1 as a reference value
349 (Christophe et al., 2008), therefore only 16 parameters are included in the
350 sensitivity analysis and estimation procedure.

351 The non-linear generalized least squares method with Gauss Newton al-
352 gorithm for optimization (Cournede et al., 2011) was used for estimating the
353 16 parameters of four genotypes. The target field data include *(i)* total blade
354 mass, total petiole mass, total internode mass, and capitulum mass, all col-
355 lected once a week during 15 weeks in total, and *(ii)* individual blade mass.
356 Regarding the target field data at organ scale used for parameter estimation,
357 only individual blade area data was available. All organs were only weighted
358 at compartment scale. In particular, independent blade mass data was not
359 available, while these data are required for a better estimation of SUNLAB
360 parameters. Therefore, profiles of individual blade mass were estimated as
361 follows: at each date when total blade mass and total blade areas were mea-
362 sured at compartment level, a virtual SLA value was computed as the ratio
363 of these two quantities and was used to generate a set of individual blade
364 mass from the sequence of areas. The model can thus be viewed as a dynamic
365 interpolation solver that generates both blade areas and mass between those
366 fixed measurement dates. Since these measurements at individual scale were

367 performed 6 times, the estimated blade mass represent around 150 data for
 368 each genotype, to be added to the 60 data at compartment scales, giving a
 369 total of around 210 observation data used for the parameter estimation of
 370 each genotype.

371 A sensitivity analysis was performed on SUNLAB parameters to under-
 372 stand their relative influence on determining the main model output, the
 373 yield Y . A global method was used, the Sobol method (Saltelli et al., 2000;
 374 Wu and Cournede, 2010). In this method, parameters are considered as
 375 random variables that are drawn from predefined distributions, chosen here
 376 as uniform distributions since no *a priori* knowledge is available for the 16
 377 SUNLAB parameters. Plausible interval boundaries are defined: the lower
 378 boundary is set as 0.5 times of the parameter's minimum estimated value
 379 among all genotypes, and the upper boundary is set as 1.5 times of the pa-
 380 rameter's maximum estimated value. This allows computing an estimator
 381 of the output variance, $V(Y)$. The first-order sensitivity index of a given
 382 parameter X_i can thus be defined as:

$$S_i = \frac{V_{X_i}(E_{\sim X_i}(Y|X_i))}{V(Y)} \quad (17)$$

383 where the inner expectation operator is the mean of Y taken over the possible
 384 values of all other parameters except X_i ($E_{\sim X_i}$) while keeping X_i fixed. Then
 385 outer variance is taken over all possible values of X_i . Similarly, higher order
 386 sensitivity indices can be defined to characterize the effects of interactions
 387 between parameters on the output variance. Sensitivity indices are normal-
 388 ized thanks to the well-known formula of variance decomposition. Here, 1000
 389 parameter sets are generated from the Sobol sequence in the calculation.

390 This crop model SUNLAB and the statistical analysis methods are inte-
391 grated in the platform PYGMALION (Cournède et al., 2013): this platform
392 is currently developed and used in the laboratory of Applied Mathematics
393 and Systems at Ecole Centrale Paris, and is available to a few other labs for
394 collaborative research projects. Programmed in C++ computer language, it
395 is dedicated to the mathematical analysis of plant growth models, including
396 the parameter estimation and sensitivity analysis methods used in this pa-
397 per. It comprises approximately 20 classical and new models of plant growth,
398 among which are Greenlab (Hu et al., 2003), PILOTE (Mailhol et al., 1997,
399 2004), STICS (Brisson et al., 1998), SUNFLO (Casadebaig et al., 2011) and
400 SUNLAB.

401 **3. Results**

402 *3.1. Sensitivity analysis*

403 A sensitivity analysis was performed on the 16 parameters (described in
404 2.3) of SUNLAB for the yield, using the Sobol method of variance decompo-
405 sition. Results are gathered in Table 2 for the most influential parameters.
406 The sum of all first order indices was 0.87, which means that the part of
407 variance due to parameter interactions was less than 15%: this justifies that
408 the sensitivity analysis of this model can be grounded on first-order indices
409 of parameters. The most influential parameters are those driving the dynam-
410 ics of capitulum sink variations, $sinkA(cap)$ and $sinkB(cap)$, accounting for
411 51% and 12% respectively of the yield variance. The only other parameter
412 with significant sensibility index is a parameter of internode sink variation,
413 $sinkA(intern)$. All other parameters account for less than 5% of the yield

414 variance. This result suggests that dynamics of biomass allocation to the
415 capitulum, more than the value of its sink, are important for yield determi-
416 nation.

417 [Table 2 about here.]

418 3.2. Model parameterization

419 3.2.1. Parameter estimation for four sunflower genotypes

420 The SUNLAB parameters were estimated for the four different geno-
421 types (“Albena”, “Melody”, “Heliasol”, and “Prodisol”) using experimental
422 datasets of “2001” (non-limiting conditions) and “2002a” (with water deficit).
423 The values of the 12 sink competition related parameters are shown in Table
424 3 with the associated standard deviation.

425 These parameter values were independently estimated for each genotype,
426 *i.e.* no *a priori* genotypic correlations were imposed. This allows comparing
427 the genotypes according to their parameter values. The standard error could
428 allow testing the significance of differences between two parameter values, but
429 this would only be an approximate result since the number of observations
430 that directly influence the estimation of each parameter was unknown. **to**
431 **change with the results of the test.** Qualitative observations can nevertheless
432 be done. For example, blade parameter $sinkA(blade)$ in the sink variation
433 function of blades appears significantly different between four genotypes,
434 while no clear evidence of genotypic variability was found for capitulum sink
435 strength ratio $SR(capitulum)$ (see also Fig. 4). The internode sink ratio,
436 $SR(internode)$, was found different for genotypes “Albena” and “Melody”,
437 but took similar values for “Heliasol” and “Prodisol”.

438

[Table 3 about here.]

439 *3.2.2. Model performances: reproducing genotype-induced variability*

440 Even when grown under non-limiting controlled conditions, the four stud-
441 ied varieties presented some phenotypic variability, that might be intrinsically
442 regulated by genotypic influences. This phenotypic variability was in partic-
443 ular observed on daily radiation interception efficiency $RIE(d)$, total blade
444 area $AA(d)$, leaf number $N(d)$, cumulated dry biomass $CDM(d)$ and biomass
445 partitioning. This is illustrated in Fig. 3 for dry mass compartments (blade,
446 internode and capitulum) with the “2001” experimental dataset. This figure
447 also illustrates the model ability to reproduce this (presumably) genotypic
448 variability.

449

[Figure 3 about here.]

450 The estimated parameter values (Table 3) allow tracking back the dy-
451 namics of biomass allocation and analyzing the internal mechanisms under-
452 lying sink competition. For instance, compared to “Prodisol”, blades of
453 “Albena” entered earlier in the competition for biomass but the capitulum
454 reached its maximum demand later (Fig. 4): this may explain that in the
455 end “Albena” had bigger total blade biomass but smaller capitulum biomass
456 than “Prodisol” (Fig. 3). Genotypic characterization can also come from the
457 biomass accumulation module: “Melody” had larger internode and capitu-
458 lum biomass than “Heliasol”, and they had similar blade biomass, as can
459 be seen in Fig. 3. This was due to a higher radiation use efficiency of the
460 “Melody” genotype.

461

[Figure 4 about here.]

462 3.2.3. Model performances: reproducing environment-induced variability

463 The SUNLAB model was calibrated using “2001” and “2002a” exper-
464 imental datasets that included data for plants grown without water deficit
465 (“2001”) and plants grown under water deficit (“2002a”). The parameterized
466 SUNLAB model was able to simulate the phenotypic variability induced by
467 the two contrasted environmental conditions of “2001” and “2002a” datasets.
468 This is illustrated in Fig.5 that shows experimental data and simulations of
469 radiation interception efficiency $RIE(d)$, total blade area $AA(d)$, leaf number
470 $N(d)$, cumulated dry above-ground biomass $CDM(d)$ and biomass compart-
471 ments (capitulum, blades, petioles, internodes) for the “Melody” genotype.
472 It can be noticed that “Melody” was not very sensitive to water stress since
473 the dry mass accumulation did not significantly vary. Graph B shows that
474 there were under-estimations of total blade area. This was due to the mod-
475 eling equations of leaf area (see equation 6 and equation 7). These equations
476 are inherited from SUNFLO model and define a common formula for all geno-
477 types to calculate total leaf area based on genotype-specific parameters $A2$
478 and $A3$. This common formula does not allow to account for all the genotypic
479 variance of total leaf area: possible improvements on this part of the model
480 are discussed in section 4. Graph E and Graph F of this Fig.5 present some
481 details on two other genotypes: biomass compartments of “Prodisol” and in-
482 dividual blade mass profile for “Heliasol”. Water stress induced a decrease in
483 the capitulum biomass of “Prodisol” plants, despite a slight increase in blade
484 biomass. The effect of water stress can also be observed on the individual
485 blade mass profile of “Heliasol” plants: blades on the last ranks grew less in
486 water deficit conditions (“2002a”) than in standard conditions (“2001”).

487

[Figure 5 about here.]

488 *3.3. Model evaluation*

489 In order to test the model predictive ability, SUNLAB was confronted
490 to an additional experimental dataset “2002b”, that was not used for the
491 parameterization step. Fig.6 presents some phenotypic traits for the “Al-
492 bena” genotype: for total blade areas and radiation interception efficiency,
493 data were underestimated by model predictions, total dry biomass was also
494 proportionally affected, but the results were reasonable for the biomass com-
495 partment dynamics. The root mean square error (RMSE) of organ mass
496 for genotype “Albena”, calculated on days with available experimental data,
497 was 36.4 and its coefficient of determination was 0.95. However, it has to be
498 noticed that this evaluation process was still at a preliminary step since our
499 additional experimental dataset “2002b” was measured in experimental con-
500 ditions similar to those of the “2002a” dataset which was used to calibrate
501 the model.

502

[Figure 6 about here.]

503 *3.4. Model Application: an exploratory study on specific leaf area*

504 Specific leaf area (SLA) is an important variable in plant growth mod-
505 eling. In most dynamic models, it is usually used to determine blade sur-
506 face area values from blade biomass, as in GREENLAB (Christophe et al.,
507 2008) or in TOMSIM (Heuvelink, 1999). Since blade area in turn determines
508 the biomass production, accurate estimation of SLA is mentioned as a ma-
509 jor source of error in models and implies difficulties in obtaining a reliable
510 computation of leaf area index, which is the main component of biomass

511 production modules (Heuvelink, 1999; Marcelis et al., 1998). It is however
512 generally considered as constant, although it has been shown, for instance
513 on wheat (Rawson et al., 1987), that SLA varies according to genotypes,
514 leaf ranks and leaf growing periods. Regarding sunflower, the variations of
515 SLA and the factors influencing them are still poorly known. As SUNLAB
516 can simulate dynamics of individual blade mass profiles independently from
517 those of blade areas, the SLA can be computed as a model output, contrary
518 to the classical situation where it is taken as input. In Fig.7, the simulated
519 and observed values for individual blade areas and masses of “Melody” in
520 the “2001” dataset are displayed for each blade rank and six different growth
521 stages.

522 [Figure 7 about here.]

523 The SLA was computed at the time when individual blades have reached
524 their highest mass on 67th day. SLAs are illustrated for blades ranking from
525 9 to 15 which are those whose individual blade mass and area had the best
526 accordance to the field data (Fig. 7). The root mean squared error (RMSE)
527 of SLA for these blades ranking from 9 to 15 was 11 and the coefficient of
528 variation (CV) was 25%. But for all blades on 67th day, including those
529 whose individual blade leaf areas were poorly simulated, the RMSE of SLA
530 for genotype Melody became 35, with CV value 76%. The computed SLA
531 showed some variability among the four genotypes. But since the current
532 SUNLAB parameters came from reconstructed individual blade masses, these
533 simulated SLA results are expected to be improved with better experimental
534 data in the future. Moreover, the modeling of individual leaf area should be
535 improved as well for more accuracy on this result.

536 4. Discussion and conclusion

537 *Models in the breeding process.* After further tests and improvements, this
538 new SUNLAB model should present robust enough predictive capacities and
539 ability to differentiate between genotypes in order to be proposed as a proper
540 tool for the understanding of crop phenotypes induced by genotype \times en-
541 vironment interactions. Practical considerations should also be examined
542 in our context of model application, *i.e.* transferring model-based informa-
543 tion to breeders. This kind of information could be for instance recommen-
544 dations on optimal environmental conditions or management practices for
545 a given genotype; the identification of particular features (a subset of the
546 model parameters, for instance) to focus on in the breeding process in order
547 to create variants with some targeted traits; environmental characterization
548 for genotypes performances; or the prediction of crop growth and harvest.

549 SUNLAB has the potential to be used in studying the link between crop
550 model parameters and genetic information. As stated in Messina et al.
551 (2006), the breeding of higher-yielding crop plants would be greatly accel-
552 erated if the phenotypic consequences of changes at some genetic markers
553 of an organism could be reliably predicted. Recently, quantitative trait loci
554 (QTL) information has been incorporated into some organ-level crop models
555 (Reymond et al., 2003; Yin et al., 2006; Xu et al., 2011). To address the
556 link between model parameters and QTL, well designed models and suit-
557 able experimental data are required. Appropriate model structures allow
558 sufficient physiological feedback features to be incorporated. Model input
559 parameters should be designed to be grounded potentially in gene-level un-
560 derstanding (Yin et al., 2004). It requires the plant growth model parameters

561 having biological meaning to represent genetic coefficients (Yin and Struik,
562 2010; Tardieu, 2003). The organ-level model SUNLAB and its parameters
563 are expected to meet the requirements. In line with what has been done
564 for pepper in Alimi et al. (2013), SUNLAB is considered to be used in a
565 study with an experimental database of 90 sunflower genotypes which are
566 F1 hybrid of the first filial generation resulting from a cross mating of 9 ×
567 10 distinctly different parental types. After estimating SUNLAB parameters
568 for the 90 genotypes, statistical analyses of the correlations between different
569 genotypes’ parameters could reveal certain genetic links.

570 *About the modeling approach: from process-based model to functional struc-*
571 *tural model.* The design of the SUNLAB model was based on an ecophys-
572 iological model, SUNFLO, that was transformed to a FSPM and enriched
573 with a mechanistic module for biomass allocation to organs. Fenni: in the
574 deleted paragraph “While there exist many excellent PBM models with ac-
575 curate model identification and growth description, it is possible to convert
576 them into FSPMs to take advantage of FSPMs’ structures and organs’ in-
577 teraction, and to reduce the efforts of building a FSPM from blank. Feng
578 et al. (2010) tested using GREENLAB sink-source solver to improve the PBM
579 model PILOTE (Mailhol et al., 1997) for the crop Maize (*Zea mays* L.) Ac-
580 tually, these previous sentences were already re-used below.. In this paper,
581 SUNLAB is a good demonstration for the crop Sunflower (*Helianthus an-*
582 *nuus* L.). It defines sunflower’s structural development and it adds complex
583 biomass partitioning mechanism to SUNFLO, while it keeps certain modules
584 of this PBM model, with the advantages of inheriting its ecophysiological
585 merits...”, some sentences were actually trying to answer the first reviewer’s

586 question in the previous review: “ A simple conceptual representation could
587 be useful to better understand how the source-sink model (GREENLAB)
588 integrates with process-based model (SUNFLO)”. Do you think we should
589 add some more sentences as the conceptual representation of the integration
590 of FSPM module in SUNLAB?Vero: I am not sure, but I think that what
591 the reviewer meant was that we add a figure with a diagramm of the SUN-
592 LAB model, don't you think so? If so, anyway, we have not done it. In
593 process-based models (PBM), plants are usually considered only at the level
594 of organ compartments. Turning them into FSPM allows taking advantage
595 of the simulation of individual organs' growth and of interactions between
596 organogenesis and functioning. FSPMs focuses on the development, growth
597 and function of individual cells, tissues, organs and plants in their spatial and
598 temporal contexts (Godin and Sinoquet, 2005). It is a solution to take into
599 account the plant's architectural development and to extrapolate PBM at
600 organ level by merging the botanical knowledge on plant development with
601 the functional equations (de Reffye et al., 2008). Introducing a mechanism
602 of trophic competition at organ level in a PBM, as done in this study, opens
603 the possibility to model feedbacks effects of biomass partitioning on other
604 processes such as photosynthesis or organogenesis (Mathieu et al., 2009).

605 A more classical way to construct FSPM consists in integrating function-
606 ing processes into an existing architectural model. This was done for instance
607 for trees in the AMAP- suite (Barczi et al., 2008), for grappevine in Pallas
608 et al. (2011) based on the relationships defined for organogenesis in Lebon
609 et al. (2004), or for wheat in Evers et al. (2010) who built a FSPM from
610 the ADEL-wheat model. Once plant architecture is simulated, incorporating

611 functional processes arise as a natural subsequent step in model development.
612 In particular, these 3D-mock-ups are often used to compute light interception.
613 In contrast, since SUNLAB originates from a PBM, the emphasis is
614 put on modeling plant functioning, phenology and effects of water and ther-
615 mal stresses, while light interception is modeled in a rather simplistic way
616 not relying on the exact 3D structure. A similar approach was applied for
617 the development of the Ecomeristem model of rice growth (Luquet et al.,
618 2006) that incorporates some features (carbon supply, simulation of an ini-
619 tial carbon reserve pool and the mobilisable fraction thereof) of a simple crop
620 model SARRA-H (Dingkuhn et al., 2003). Feng et al. (2010) also tested us-
621 ing the GREENLAB sink-source solver to improve the PBM model PILOTE
622 (Mailhol et al., 1997) for the crop Maize (*Zea mays* L.).

623 Generally, our approach fits into a current general trend of development
624 of modular models, with generic modules that can be shared by other mod-
625 elers. This trend goes hand in hand with the increasing number of modeling
626 platforms: Pygmalion in our case (Cournède et al., 2013), OpenAlea (Pradal
627 et al., 2004), GroIMP (Kniemeyer et al., 2006), etc. These platforms pro-
628 vide flexible frameworks for the coupling of models or the re-use of modules
629 in different models. It reduces the efforts of building models from blank
630 and mutualizes the implementation work. SUNLAB falls within that trend
631 since most of its modules are generic and could be easily adapted to other
632 crops (e.g. biomass allocation module, biomass production module, water
633 budget,...).

634 *Mechanistic modeling and empirical modeling.* SUNLAB is the fruit of an ef-
635 fort to make the SUNFLO model more mechanistic (through the modeling of

636 biomass partitioning). Mechanistic models generally arise from approaches
637 relating to the complex system theory: they consider the individual com-
638 ponents of the system and their interactions, and what emergent properties
639 appear. They have the potential to be used out of their calibration inter-
640 val, provided that the model predictive capacities have been preliminarily
641 checked. In contrast, empirical models are derived on direct descriptions of
642 observed data. They are usually regression based and provide a quantitative
643 summary of the observed relationships among a set of measured variables.
644 Most plant growth models combine in fact both modeling approaches as a
645 mixture of mechanistic modules and empirical modules.

646 It is expected that mechanistic description of ecophysiological processes
647 improves the model predictive capacities and their ability to differentiate be-
648 tween genotypes (Allen et al., 2005; Minchin and Lacoïnte, 2005; Bertheloot
649 et al., 2011). However, the extent to which more mechanistic models are
650 necessarily better should be questioned. In particular, since the parameters
651 in mechanistic modules are assumed to have assigned biological meanings
652 and to represent properties of real system components, the reliability of the
653 underlying assumptions need to be carefully validated. I kept this sentence,
654 but I am not sure of what you meant, Fenni. Could you explain me? Fenni:
655 because the mechanistic models normally try to simulate the biological hy-
656 pothesis, the parameters in mechanistic modules have assigned biological
657 meanings. Therefore, it need more scrutiny to determine whether the hy-
658 pothesis and the biological meanings are true. I got this sentence from this
659 article: Biomedical Applications of Computer Modeling, Chapter 7.2 Em-
660 pirical or mechanisticvro: ok. Do you agree with the way I modified the

661 **previous sentence, then?** Thus, the appropriateness of mechanistic models
662 needs close scrutiny (Christopoulos and Michael, 2000). Moreover, the pa-
663 rameterization effort of these more and more complex models should always
664 be taken into account when improving their mechanistic description, to pre-
665 vent from a high level of uncertainty in the parameters which may hinder the
666 original purposes of the model in terms of prediction and genotypic differen-
667 tiation. So, as stated in the introduction, a delicate trade-off has to be found
668 between mechanistic aspects and complexity, in order to provide proper tools
669 that might be used in the breeding context.

670 *Parameter estimation issue: direct measurements and model inversion.* Two
671 kinds of methods were involved for SUNLAB parameterization: estima-
672 tion through direct measurements and estimation through statistical meth-
673 ods, sometimes referenced as model inversion methods. Direct measurement
674 method enables direct access to the desired parameter via experimental mea-
675 surements (Jeuffroy et al., 2006). The model inversion method, involving
676 mathematical and statistical calculations, estimates one or more parame-
677 ters by confronting observed data to simulation results (Guo et al., 2006;
678 Cournede et al., 2011).

679 Direct measurement is used to estimate parameters that have biological
680 meanings, and that can be directly observable or easily calculated from mea-
681 sured indicators. Parameters with biological meanings consist of two types:
682 “genotypic parameters” which differ between varieties and “crop parameters”
683 which are parameters with small variance among all genotypes. Theoretically,
684 direct measurement method is the best for estimating genotypic parameters
685 and consequently for genotype characterization. The breeder could measure

686 it directly on lines under development in experiments in order to predict the
687 expected effects (Reymond, 2001). Similarly crop parameters can be mea-
688 sured directly from field data. Because of the direct and accurate measures on
689 elementary processes, these estimated parameters have advantages in terms
690 of ecophysiological relevance, parameter accuracy and genotype characteriza-
691 tion, compared with model inversion method. This perspective has led to au-
692 tomated and high-throughput advanced plant phenotyping (see for example
693 Granier et al. (2005), Sotirios and Christos (2009)). However, the accurate
694 elementary processes do not necessarily imply that the combination of these
695 processes will provide the same accuracy at plant scale. The nonlinear in-
696 teractions between processes as well as the necessary simplifications in terms
697 of the number of ecophysiological processes considered in the model make
698 the whole plant model not a simple combination of the elementary models
699 that were well calibrated by experiments: plants are complex systems whose
700 description of elementary process interactions, plasticity and robustness re-
701 mains an open issue (Yin and Struik, 2010). Therefore, parameterization
702 methods relying on model inversion to estimate parameters from experimen-
703 tal data at organ or whole plant levels offers an alternative. This method can
704 ensure an optimized fitting error on training data, but the prediction error
705 on validation data has to be carefully checked to avoid over-fitting problems.
706 The parameters thus obtained have the risk to be less relevant for their bio-
707 logical meanings than direct measurement, because these parameters values
708 may be altered by the error compensation from fitting whole plant processes
709 and from other simultaneously estimated parameters (Jeuffroy et al., 2006).
710 They nevertheless characterize the plant global behavior and may still be

711 used to differentiate between genotypes (Letort, 2008).

712 When parameter estimation is demanded for a high number of genotypes,
713 direct measurement method becomes impractical, because this method often
714 requires specific trials and measurements, which are complicated, costly and
715 even impossible to implement sometimes (Reymond, 2001). Routine mea-
716 surement of these parameters for a large number of varieties may also pose
717 a problem, particularly when measurements require special equipment and
718 controlled condition experiments (Jeuffroy et al., 2006). Model inversion
719 method is adopted for these cases because it is experimentally less costly
720 and less time-consuming. For instance in most dynamic models, the direct
721 measurement method would often require frequent measurement points (e.g.
722 daily), while with the indirect method, data can be collected only at some
723 given time points and still allow the modellers to retrieve the past growth of
724 the crop. Parameters can even be estimated from very limited sets of data
725 (Kang et al., 2011).

726 Moreover, some parameters are “hidden”, i.e. cannot be experimentally
727 measured and can only be estimated by model inversion method. They usu-
728 ally appear in mechanistic modules, because their underlying mechanisms
729 can produce emergent properties that can be difficult to disentangle *a pos-*
730 *teriori* from the resulting phenotype. It also implies that, because of their
731 interactions, these kinds of parameters cannot be obtained independently
732 from each other: the whole estimation process needs to be performed on all
733 the data at the same time (it is not possible to optimize sequentially on data
734 for different types of organs, for instance).

735 In SUNLAB, the parameters inherited from SUNFLO have biological

736 meaning and had been measured for 20 genotypes. Meanwhile, the param-
737 eters involved in the new biomass allocation module are hidden parameters
738 that can only be estimated by model inversion, because the biomass alloca-
739 tion process at organ level is difficult to observe and to be directly measured.

740 *Limitations and perspectives*

741 *Modeling.* From the model performances results, we can see that the mod-
742 eling of blade area needs to be uppermost improved in SUNLAB. A first
743 improvement could consist in replacing the use of the logistic function by a
744 fully mechanistic approach including modeling the SLA instead of deriving it
745 *a posteriori* from the simulated mass and areas. Thereby, feedbacks effects of
746 trophic competition on leaf area expansion could be explored and modeled.

747 The biomass accumulation module was directly inherited from SUNFLO
748 that has been tested in different environmental conditions for 26 genotypes
749 (Casadebaig et al., 2011; Lecoeur et al., 2011) and is in line with what is classi-
750 cally done in models of the same class as SUNLAB (e.g. Tomsim (Heuvelink,
751 1999), Ecomeristem (Luquet et al., 2006)). A more detailed approach, at
752 individual leaf level, could be considered by computing the amount of inter-
753 cepted radiations: several methods are available (e.g. Nested Radiosity light
754 model in Evers et al. (2010) or a Monte-Carlo radiation model in Xu et al.
755 (2011)) but they require an accurate modeling of the plant structure which is
756 currently not available and would necessitate additional experimental work
757 to be parameterized. It has to be noted that SUNLAB is not *stricto-sensu* a
758 FSPM since no 3D shape is simulated.

759 As regards the biomass distribution module that was introduced in our
760 study, our approach is based on the concept of common pool of assimilates

761 and relative sink competition. However, some other models (e.g. ECOPHYS
762 [Lacointe et al., 2002])) and experimental observations (Pallas et al. (2008))
763 suggest that the distance from source to sink could have an influence. An al-
764 ternative approach is thus to consider transport-resistance methods, as done
765 for instance in the L-PEACH model [Allen et al., 2005]: although these meth-
766 ods are biologically more relevant, they are generally complex and the result-
767 ing biomass distribution remains highly dependent on the determination of
768 sink activity. Bancal and Soltani [2002] compared the partitioning coeff-
769 cients obtained from an improved version of the transport-resistance model
770 of [Minchin et al., 1993] to the classical sink-based partitioning model: they
771 concluded that the resistance to flux propagation has an influence only in
772 pathologic cases of very low source activity and that resistance terms could
773 be abandoned in most cases as they are only a mathematical burden whose
774 parameter values are very difficult to measure experimentally. In our source-
775 sink approach, the main limiting factor is not the geometrical distance but
776 the topological organization of source and sinks (i.e. the number of other
777 sinks in a source-sink pathway) (Letort, 2008).

778 **what do you mean exactly, with this solution?**Fenni: I mean the feedback
779 effects of trophic competition on other plant functions could be simulated
780 in the future. It was written in the paragraph you deleted as such “How-
781 ever, the lack of trophic competition simulation may hinder the simulation of
782 feedback effects of biomass partitioning on other processes. As Pallas et al.
783 (2008) state, trophic competition influenced the organogenesis of grapevine
784 in their research. They suggest that a modeling approach simulating sink
785 strength variation and the local effects of sink proximity would be more rele-

786 vant than a model considering only development as a function of thermal time
787 or the global distribution of available biomass”. I tried to write the modeling
788 limitations in term of blade area modeling, and the modeling of feedback ef-
789 fects of trophic competition. Besides, the third reviewer asked in last review
790 “why the biomass accumulation is a very global level compared to the organ
791 level elsewhere. How do you justify these differences?” I answered him that
792 “The biomass accumulation module is directly inherited from SUNFLO while
793 the biomass distribution module is completely changed, as the first step of
794 adapting it into a FSPM model. Its performance and evaluation have shown
795 satisfactory results. Next step will be to add feedback effects of biomass
796 partitioning to the model, which will improve the simulation of morphogen-
797 esis, biomass production etc. This point is discussed in the Discussion and
798 conclusion session in this new version of paper”. Therefore I discussed here
799 why feedback effects need to be simulated. This is also my answer to the
800 first reviewer’s question “where is the biomass production’s under-estimation
801 from” and “why the upper leaves’ SLA can not be well simulated”. I put
802 the reasons to the bad simulation of blade area, especially the upper leaves’
803 blade area. I mentioned some improvements of biomass production modeling
804 can be planned in the future, such as the feedback effects of biomass distribu-
805 tion on blade area modeling, and also the consequent simulation of biomass
806 production. I also mentioned that to improve the simulation of SLA, “Be-
807 sides the approach that the logistic function, which is used to model leaf area
808 in SUNLAB, can be compared with other functions, the feedback effect of
809 trophic competition on leaf area expansion can be investigated and modeled.”
810 So to sum up, with the limitation of blade area modeling, I tried to answer

811 reviewers' three questions: 1, why the biomass production is a very global
812 level compared with biomass distribution; 2, where is the under-estimation
813 of biomass production from; 3, why did we state that the SLA simulation of
814 upper leaves are not well simulated.

815 Fenni: the deleted sentences of leaf senescence “In SUNLAB, leaf senes-
816 cence is modeled to occur between phenology stages *M0* and *M3*. The
817 phenology timing “CTT(d)” is affected by water stress, which affects con-
818 sequently the rate of leaf senescence. Its leaf senescence start time can be
819 better modeled, since sunflower leaves senescence may occur before *M0* stage
820 in drought stressed conditions”, is actually an answer to the second reviewer’s
821 question in previous review: “Leaf senescence is in the model expected to
822 occur between the stages *M0* and *M3*. In the SUNLAB model, the impact
823 of the drought stress on the phenology is taken into account (page 6-line 54
824 to page 7-line 20); however this point should benefit to be discussed, as sun-
825 flower leaves senescence may occur before the *M0* stage in drought stressed
826 conditions”. I tried to mention the limit of leaf senescence modeling. Sunlab
827 doesn't simulate leaf senescence in strong stress, occurring before *M0*. **Ok,**
828 **I put some back, then. Do you agree?** Besides, leaf senescence is currently
829 affected by water stress only (through the phenology timing “CTT(d)” that
830 affects consequently the rate of leaf senescence) and occurs between phenol-
831 ogy stages *M0* and *M3* while, in reality, it may occur before *M0* stage in
832 severe drought conditions. Therefore, the SUNLAB leaf senescence may need
833 also modifications and could include the effects of other environmental cues
834 such as day length and temperature, and various biotic and abiotic sources of
835 stress, that can affect the initiation and progress of leaf senescence (Aguera

836 et al., 2012).

837 *Sensitivity analysis.* The sensitivity analysis of SUNLAB model in this arti-
838 cle has provided parameters' accountability to the variance of crop yield and
839 revealed less than 15% of effects of parameter interactions in biomass dis-
840 tribution module. It suggests that for the simulation of yield, the empirical
841 modeling could be reasonable, i.e. calculating the yield without the con-
842 sideration of interactions between the capitulum and other organs' growth.
843 However, the dominant influence of capitulum's sink strength dynamics pa-
844 rameters $sinkA(cap)$ and $sinkB(cap)$ may indicate that a better harvest
845 function should be tested rather than a linear relationship with total dry
846 biomass. Sensitivity analysis could also be performed on other output of in-
847 terest such as blade area or stem biomass, in order to better understand the
848 respective influence of the input parameters on the different components of
849 plant phenotype. A sensitivity analysis considering all SUNLAB parameters,
850 rather than only parameters in biomass distribution, is also necessary to dis-
851 cover the potential interactions existing among all parameters and modules.
852 A limitation of the Sobol method that was used for these sensitivity analyses,
853 is that no correlations were included between the parameters, although they
854 might certainly exist. For example, the correlation analysis of these param-
855 eters based on our estimated values in a family of four genotypes indicates
856 a correlation factor of 0.8 for parameters $SR(petiole)$ and $SR(internode)$.
857 For the further characterization of genotypes, sensitivity techniques designed
858 for taking into account input parameters correlations should be adopted (Xu
859 and Gertner, 2007; Chastaing et al., 2012; Wu et al., 2013).

860 *Model parameterization and evaluation.* Once calibrated, SUNLAB was able
861 of reproducing phenotypic variabilities in different genotypic and environ-
862 ment experiments scenarios. The genotypes “Melody” and “Heliasol” (Fig. 3)
863 were shown to have better drought tolerance than the two other genotypes.
864 Their yields were hardly not influenced by water stress while the other two
865 experienced a slight reduction (around 15% of 2001 harvest). With some vari-
866 ation according to plant species, certain stages such as germination, seedling
867 or flowering are known to be the most critical stages, vulnerable to water
868 stress (Hadi et al., 2012). Seed germination is the first critical stage and
869 the most sensitive in the life cycle of plants (Ahmad et al., 2009) and seeds
870 exposed to unfavorable environmental conditions, such as water stress at this
871 stage may have seedling establishment compromised (Albuquerque and Car-
872 valho, 2003). However our simulation and field data suggested that drought
873 stress had little effect on crop growth. As sunflower is categorized as a low to
874 medium drought sensitive crop (Turhan and Baser, 2004), the water deficit
875 level might not be strong enough to cause severe growth deficits. An environ-
876 mental scenario with stronger water deficiency would be required to better
877 parameterize the model. Then, additional scenarios (more cultivar/lines or
878 different kinds of stress conditions) could either help further quantifying the
879 model predictive ability and the range of its validity conditions, or help iden-
880 tifying the inappropriate or missing modules that need further investigation.
881 More importantly, since the model parameters are numerically estimated,
882 these additional scenarios will also allow testing their stability under differ-
883 ent environmental conditions and using phenotyping data at different growth
884 stages (Ma et al., 2007, 2008). A good stability is a necessary condition to

885 consider these parameters as genotype-dependent and to move forward in-
886 vestigating their potential genetic determinism, as illustrated for example in
887 (Buck-Sorlin et al., 2005).

888 Fenni: Ok, I agree. This paragraph was added because of the first re-
889 viewer’s question “ Results from model evaluation are not really discussed.
890 I mean, all model are wrong but it is needed to discuss how suitable they
891 are for their use. e.g. Does improving the phenotyping (more cultivar/lines,
892 stress scenarios) automatically increase the prediction capacity when param-
893 eter are numerically estimated? Any insights on the actual model perfor-
894 mance for discriminating cultivars Vs working with lines?”. I didn’t answer
895 him about “discrimating cultivars” vs “working with lines”, because I don’t
896 know the answer. I think in our model, we don’t have parameters which can
897 discriminate lines. We only have genotypic parameters, which are cultivar-
898 dependant, and common parameters for all genotypes. He didn’t pose any
899 further question about this point in the new letter, but maybe you could add
900 something to answer his previous question. Ok, see above: I have added the
901 sentences from ”“Then, additional scenarios...”’: do you agree?”’

902 *Conclusion: Summary of results.* A functional-structural model SUNLAB
903 was developed. It describes the sunflower topology and morphogenesis at
904 organ level with blades, petioles, internodes, and capitulum. Coordination
905 of the expansion dynamics of these organs is ruled by their initiation and
906 senescence thermal times. Ecophysiological processes interact with plant
907 structural dynamics to affect biomass accumulation and partitioning to or-
908 gans. As a joint concept of GREENLAB and SUNFLO models, SUNLAB
909 has better structural features than SUNFLO and it succeeds to deal with the

910 biomass distribution at organ level. SUNLAB inherits the ecophysiological
911 merits of SUNFLO that have been validated in different environmental con-
912 ditions for 26 genotypes (Casadebaig et al., 2011; Lecoeur et al., 2011). In
913 contrast, GREENLAB over-simplifies a number of processes, such as photo-
914 synthesis and assimilate conversion to biomass (Guo et al., 2006; Ma et al.,
915 2008), and it is still in its preliminary stage to include water source influence
916 and root system (Li et al., 2009). The ability of this newly-developed SUN-
917 LAB model to reproduce observed data of sunflower growth was evaluated
918 on four genotypes “Albena”, “Melody”, “Heliasol” and “Prodisol”.

919 Aguera, E., Cabello, P., Mata, L., Molina, E., Haba, P., 2012. Metabolic
920 regulation of leaf senescence in sunflower (*helianthus annuus l.*) plants,
921 senescence. *Agricultural and Biological Sciences*.

922 Ahmad, S., Ahmad, R., Ashraf, M., Ashraf, M., Waraich, E., 2009. Sun-
923 flower (*helianthus annuus l.*) response to drought stress at germination
924 and seedling growth stages. *Pak J Bot* 41 (2), 647–654.

925 Albuquerque, F., Carvalho, N., 2003. Effect of type of environmental stress on
926 the emergence of sunflower (*helianthus annuus l.*), soyabean (*glycine max*
927 (*l.*) merril) and maize (*zea mays l.*) seeds with different levels of vigor. *Seed*
928 *Sci Technol* 31, 465–467.

929 Alimi, N. A., Bink, M. C. A. M., Dieleman, J. A., Nicolai, M., Wubs, M.,
930 Heuvelink, E., Magan, J., Voorrips, V., Jansen, J., Rodrigues, P., Heij-
931 den, G., Vercauteren, A., Vuylsteke, M., Song, Y., Glasbey, C., Barocsi,
932 A., Lefebvre, V., Palloix, A., van Eeuwijk, F. A., 2013. Genetic and QTL

- 933 analyses of yield and a set of physiological traits in pepper. *Euphytica* 190,
934 181–201.
- 935 Allen, M., Prusinkiewicz, P., Dejong, T., 2005. Using L-systems for modeling
936 source-sink interactions, architecture and physiology of growing trees, the
937 L-peach model. *New Phytologist* 166, 869–880.
- 938 Allinne, C., Maury, P., Srrafi, A., Grieu, P., 2009. Genetic control of phys-
939 iological traits associated to low temperature growth in sunflower under
940 early sowing conditions. *Plant Science* 177, 349–359.
- 941 Barczi, J.-F., Rey, H., Caraglio, Y., de Reffye, P., Barthlmy, D., Dong, Q. X.,
942 Fourcaud, T., 2008. Amapsim: A structural whole-plant simulator based
943 on botanical knowledge and designed to host external functional models.
944 *Annals of Botany* 101 (8), 1125–1138.
- 945 Bertheloot, J., Cournède, P.-H., Andrieu, B., 2011. Nema, a functional-
946 structural model of n economy within wheat culms after flowering: I. model
947 description. *Annals of Botany* In press.
- 948 Brisson, N. and Mary, B., Ripoche, D., M.-H., J., Ruget, F., Nicoullaud, B.,
949 Gate, P., Devienne-Barret. F. and Antonioletti, R. and Durr, C., Richard,
950 G., Beaudoin, N., Recous, S., Tayot, X., Plenet, D. and Cellier, R., Machet,
951 J.-M., Meynard, J.-M., Delecolle, R., 1998. Stics : a generic model for the
952 simulation of crops and their water and nitrogen balances. i. theory, and
953 parameterization applied to wheat and corn. *Agronomie* 18, 311–346.
- 954 Buck-Sorlin, G. H., Kniemeyer, O., Kurth, W., 2005. Barley morphology,

- 955 genetics and hormonal regulation of internode elongation modelled by a
956 relational growth grammar. *New Phytologist* 166 (3), 859–867.
- 957 Casadebaig, P., Guilioni, L., Lecoecur, J., Christophe, A., Champolivier, L.,
958 Debaeke, P., 2011. Sunflo, a model to simulate genotype-specific perfor-
959 mance of the sunflower crop in contrasting environment. *Agricultural and*
960 *forest meteorology* 151, 163–178.
- 961 Chapman, S., Cooper, M., Podlich, D., Hammer, G., 2003. Evaluating plant
962 breeding strategies by simulating gene action and dryland environment
963 effects. *Agronomy Journal* 95, 99–113.
- 964 Chastaing, G., Gamboa, F., Prieur, C., 2012. Generalized hoeffding-sobol
965 decomposition for dependent variables-application to sensitivity analysis.
966 *Electronic Journal of Statistics* 6, 2420–2448.
- 967 Christophe, A., Letort, V., Hummel, I., Cournede, P., de Reffye, P., Lecoecur,
968 J., 2008. A model-based analysis of the dynamics of carbon balance at
969 the whole-plant level in *arabidopsis thaliana*. *Functional plant biology* 35,
970 1147–1162.
- 971 Christopoulos, A., Michael, J. L., 2000. Beyond eyeballing: Fitting mod-
972 els to experimental data. *Critical Reviews in Biochemistry and Molecular*
973 *Biology* 35(5), 359–391.
- 974 Cournede, P., Letort, V., Mathieu, A., Kang, M., Lemaire, S., Trevezas,
975 S., Houllier, F., de Reffye, P., 2011. Some parameter estimation issues in
976 functional-structural plant modelling. *Mathematical Modeling of Natural*
977 *Phenomena* 6(2), 133–159.

- 978 Cournède, P.-H., Chen, Y., Wu, Q., Baey, C., Bayol, B., 2013. Development
979 and evaluation of plant growth models: Methodology and implementa-
980 tion in the PYGMALION platform. *Mathematical Modelling of Natural*
981 *Phenomena* 8, 112–130.
- 982 de Reffye, P., Heuvelink, E., Barthlmy, D., Cournde, P.-H., 2008. Plant
983 growth models. In: Jorgensen, S., Fath, B. (Eds.), *Ecological Models*. Vol.
984 4 of *Encyclopedia of Ecology* (5 volumes). Elsevier, Oxford, pp. 2824–2837.
- 985 Dingkuhn, M., Baron, C., Bonnal, V., Maraux, F., Sarr, B., Sultan, B.,
986 Clopes, A., Forest, F., 2003. Decision support tools for rainfed crops in the
987 Sahel at the plot and regional scales, international fertilizer development
988 center and acp-eu technical centre for agricultural and rural cooperation:
989 wageningen, the netherlands Edition. Struiff Bontekes, T.E. and Wopereis,
990 M.C.S., p. 127139.
- 991 Evers, J., Vos, J., Yin, X., Romero, P., van der Putten, P., Struik, P., 2010.
992 Simulation of wheat growth and development based on organ-level photo-
993 synthesis and assimilate allocation. *Journal of Experimental Botany* 61 (8),
994 2203–2216.
- 995 Feng, L., Mailhol, J.-C., Rey, H., Griffon, S., Auclair, D., Reffye, P. D., 2010.
996 Combining a process based model with a functional structural plant model
997 for production partitioning and visualization. 6th International workshop
998 on functional-structural plant models, 41–43.
- 999 Godin, C., Sinoquet, H., 2005. Functional-structural plant modelling. *New*
1000 *Phytologist* 166, 705–708.

- 1001 Granier, C., Aguirrezabal, L., Chenu, K., Cookson, S. J., Dauzat, M.,
1002 Hamard, P., Thioux, J.-J., Rolland, G., Bouchier-Combaud, S., Lebaudy,
1003 A., et al., 2005. Phenopsis, an automated platform for reproducible phe-
1004 notyping of plant responses to soil water deficit in *arabidopsis thaliana*
1005 permitted the identification of an accession with low sensitivity to soil
1006 water deficit. *New Phytologist* 169 (3), 623–635.
- 1007 Guo, Y., Ma, Y., Zhan, Z., Li, B., Dingkuhn, M., Luquet, D., de Reffye,
1008 P., 2006. Parameter optimization and field validation of the functional-
1009 structural model greenlab for maize. *Annals of Botany* 97, 217–230.
- 1010 Hadi, H., Khazaei, F., Babaei, N., Daneshian, J. and Hamidi, A., 2012. Evalu-
1011 ation of water deficit on seed size and seedling growth of sunflower cultivars.
1012 *International Journal of AgriScience* 2 (03), 280–290.
- 1013 Hammer, G., Cooper, M., Tardieu, F., Welch, S., Walsh, B., F, F. V. E.,
1014 2006. Models for navigating biological complexity in breeding improved
1015 crop plants. *Trends in Plant Science* 11, 587–593.
- 1016 Heuvelink, E., August 1995. Dry matter partitioning in a tomato plant: one
1017 common assimilate pool? *Journal of Experimental Botany* 46 (289), 1025–
1018 1033.
- 1019 Heuvelink, E., 1999. Evaluation of a dynamic simulation model for tomato
1020 crop growth and development. *Annals of Botany* 83, 413–422.
- 1021 Hu, B., de Reffye, P., Zhao, X., Yan, H., Kang, M., 2003. Greenlab: A
1022 new methodology towards plant functional-structural model – structural

- 1023 aspect. In: Hu, B., Jaeger, M. (Eds.), Plant Growth Models and Applica-
1024 tions. Tsinghua University Press and Springer.
- 1025 Jeuffroy, M.-H., Barbottin, A., Jones, J., Lecoecur, J., 2006. Chapter 10: Crop
1026 models with genotype parameters. Working with Dynamic Crop Models,
1027 281–307.
- 1028 Kang, F., Galinier, T., Henry Cournede, P., Lecoecur, J., 2011. Parameter-
1029 ization of plant growth models to characterize genotype by environment
1030 interactions: a methodology adapted to breeding programmes. Aspects of
1031 Applied Biology, Systems Approaches to Crop Improvement 107, 161–170.
- 1032 Kang, M.-Z., Evers, J., Vos, J., De Reffye, P., 2008. The derivation of sink
1033 functions of wheat organs using the greenlab model. Annals of Botany
1034 101(9).
- 1035 Kniemeyer, O., Buck-Sorlin, G., Kurth, W., 2006. Groimp as a platform for
1036 functional-structural modelling of plants. In: Vos, J., Marcelis, L. F. M.,
1037 deVisser, P. H. B., Struik, P. C., Evers, J. B. (Eds.), Functional-Structural
1038 Plant Modelling in Crop Production. 5.-8. 3. 2006. Springer, Berlin, p.
1039 4352.
- 1040 Lebon, E., Pellegrino, A., Louarn, G., Lecoecur, J., 2006. Branch development
1041 controls leaf area dynamics in grapevine (*Vitis vinifera*) growing in drying
1042 soil. Annals of Botany 98 (1), 175.
- 1043 Lebon, E., Pellegrino, A., Tardieu, F., Lecoecur, J., 2004. Shoot development
1044 in grapevine (*vitis vinifera*) is affected by the modular branching pattern of

1045 the stem and intra and intershoot trophic competition. *Annals of Botany*
1046 93 (3), 263–274.

1047 Lecoeur, J., Poire-Lassus, R., Christophe, A., Pallas, B., Casadebaig, P.,
1048 Debaeke, P., Vear, F., Guiloni, L., 2011. Quantifying physiological de-
1049 terminants of genetic variation for yield potential in sunflower. *sunflo: a*
1050 *model-based analysis. Functional plant biology* 38(3), 246–259.

1051 Letort, V., 2008. Multi-scale analysis of source-sink relationships in plant
1052 growth models for parameter identification. case of the greenlab model.
1053 Ph.D. thesis, Ecole Centrale Paris.

1054 Li, Z., Le Chevalier, V., Cournède, P.-H., November 9-12 2009. Towards a
1055 continuous approach of functional-structural plant growth. In: Li, B.-G.,
1056 Jaeger, M., Guo, Y. (Eds.), 3rd international symposium on Plant Growth
1057 and Applications(PMA09), Beijing, China. IEEE.

1058 Luquet, D., Dingkuhn, M., Kim, H., Tambour, L., Clement-Vidal, A., 2006.
1059 Ecomeristem, a model of morphogenesis and competition among sinks in
1060 rice. 1. concept, validation and sensitivity analysis. *Functional Plant Biol-*
1061 *ogy* 33, 309–323.

1062 Ma, Y., Wen, M., Guo, Y., Li, B., Cournde, P.-H., de Reffye, P., 2008. Param-
1063 eter optimization and field validation of the functional-structural model
1064 greenlab for maize at different population densities. *Annals of Botany*
1065 101(8).

1066 Ma, Y., Zhan, Z., Guo, Y., Luquet, D., de Reffye, P., Dingkuhn, M., 2007.
1067 Parameter stability of the structural-functional plant model greenlab as

- 1068 affected by variation within populations, among seasons and among growth
1069 stages. *Annals of Botany* 99, 61–73.
- 1070 Mailhol, J., Olufayo, A. A., Ruelle, P., 1997. Sorghum and sunflower evapo-
1071 transpiration and yield from simulated leaf area index. *Agriculture Water*
1072 *Management* 35, 167–182.
- 1073 Mailhol, J., Zairi, A., Slatni, A., Ben Nouma, B., El Amami, H., 2004.
1074 Analysis of irrigation systems and irrigation strategies for durum wheat in
1075 tunisia. *Agriculture Water Management* 70, 19–37.
- 1076 Marcelis, L., Heuvelink, E., Goudriaan, J., 1998. Modelling of biomass pro-
1077 duction and yield of horticultural crops: a review. *Scientia Horticulturae*
1078 74, 83–111.
- 1079 Mathieu, A., Cournde, P.-H., Letort, V., Barthlmy, D., de Reffye, P., 2009.
1080 A dynamic model of plant growth with interactions between development
1081 and functional mechanisms to study plant structural plasticity related to
1082 trophic competition. *Annals of Botany* 103 (8), 1173–1186.
- 1083 Messina, C., Boote, K., Loffler, C., Jones, J., Vallejos, C., 2006. Chapter
1084 11: Model-assisted genetic improvement of crops. *Working with Dynamic*
1085 *Crop Models*, 309–335.
- 1086 Minchin, P., Lacointe, A., 2005. New understanding on phloem physiology
1087 and possible consequences for modelling long-distance carbon transport.
1088 *New Phytologist* 166, 771–779.
- 1089 Nooden, L. D., Guiamet, J. J., John, I., 1997. Senescence mechanisms. *Phys-*
1090 *iologia Plantarum* 101 (4), 746–753.

- 1091 Pallas, B., Loi, C., Christophe, A., Cournde, P. H., Lecoecur, J., 2011. Com-
1092 parison of three approaches to model grapevine organogenesis in conditions
1093 of fluctuating temperature, solar radiation and soil water content. *Annals*
1094 of Botany 107 (5), 729–745.
- 1095 Pallas, B., Louarn, G., Christophe, A., Lebon, E., Lecoecur, J., 2008. Influence
1096 of intrashoot trophic competition on shoot development in two grapevine
1097 cultivars (*Vitis vinifera*). *Physiologia Plantarum* In press.
- 1098 Pradal, C., Dones, N., Godin, C., Barbier de Reuille, P., Boudon, F., Adam,
1099 B., Sinoquet, H., 2004. Alea: A software for integrating analysis and sim-
1100 ulation tools for 3d architecture and ecophysiology. In: 4th International
1101 Workshop on Functional-Structural Plant Models. Montpellier, France, p.
1102 406.
- 1103 Rawson, H., Gardner, P., Long, M., 1987. Sources of variation in specific
1104 leaf area in wheat grown at high temperature. *Australian Journal of Plant*
1105 *Physiology* 14(3), 287–298.
- 1106 Reymond, M., 2001. Variabilite genetique des reponses de la croissance fo-
1107 liaire du mais a la temperature et au deficit hydrique. combinaison d’un
1108 modele ecophysologique et d’une analyse QTL. These de l’Ecole Nationale
1109 Superieure Agronomique de Montpellier, Montpellier, France, 70.
- 1110 Reymond, M., Muller, B., Leonardi, A., Charcosset, A., Tardieu, F., 2003.
1111 Combining quantitative trait loci analysis and an ecophysiological model
1112 to analyze the genetic variability of the responses of maize leaf growth to
1113 temperature and water deficit. *Plant Physiology* 131, 664–675.

- 1114 Saltelli, A., Tarantola, S., Campolongo, F., 2000. Sensitivity analysis as an
1115 ingredient of modeling. *Statistical Science* 15 (4), 377–395.
- 1116 Sinclair, T., de Wit, C., 1975. Photosynthate and nitrogen requirements for
1117 seed production by various crops. *Science* 189, 565–567.
- 1118 Sotirios, T., Christos, N., 2009. Plant phenotyping with low cost digital cam-
1119 eras and image analytics. *Information Technologies in Environmental En-
1120 gineering Environmental Science and Engineering*, 238–251.
- 1121 Tardieu, F., 2003. Virtual plants: modelling as a tool for the genomics of
1122 tolerance to water deficit. *Trends in Plant Science* 8 (1), 9–14.
- 1123 Turhan, H., Baser, I., 2004. In vitro and in vivo water stress in sunflower
1124 (*helianthus annuus l.*). *Helia* 27 (40), 227–236.
- 1125 Vear, F., Bony, H., Joubert, G., Tourvieille de Labrouhe, D., Pauchet, I.,
1126 Pinochet, X., 2003. The results of 30 years of sunflower breeding for france.
1127 *Oleagineux, corps gras* 10, 66–73.
- 1128 Wu, Q., Bayol, B., Kang, F., Lecoeur, J., Cournede, P.-H., 2013. Sensitivity
1129 analysis for plant models with correlated parameters: Application to the
1130 characterization of sun flower genotypes. 7th International Conference on
1131 Sensitivity Analysis of Model Output.
- 1132 Wu, Q., Cournede, P.-H., 2010. The use of sensitivity analysis for the design
1133 of functional structural plant models. Sixth International Conference on
1134 Sensitivity Analysis of Model Output 2 (6), 7768–7769.

- 1135 Xu, C., Gertner, G., 2007. Extending a global sensitivity analysis technique
1136 to models with correlated parameters. *Computational Statistics and Data*
1137 *Analysis* 51, 5579–5590.
- 1138 Xu, L., Henke, M., Zhu, J., Kurth, W., Buck-Sorlin, G., 2011. A function-
1139 alstructural model of rice linking quantitative genetic information with
1140 morphological development and physiological processes. *Annals of Botany*.
- 1141 Yin, X., Goudriaan, J., Lantinga, E., Vos, J., Spiertz, H., 2003. A flexible
1142 sigmoid function of determinate growth. *Annals of Botany* 91, 361–371.
- 1143 Yin, X., Struik, P., Kropff, M., 2004. Role of crop physiology in predicting
1144 gene-to-phenotype relationships. *Trends in Plant Science* 9, 426–432.
- 1145 Yin, X., Struik, P. C., 2010. Modelling the crop: from system dynamics to
1146 systems biology. *Journal of Experimental Botany* 61 (8), 2171–2183.
- 1147 Yin, X., Struik, P. C., van Eeuwijk, F. A., Stam, P., Tang, J., 2006. QTL
1148 analysis and QTLI-based prediction of flowering phenology in recombinant
1149 inbred lines of barley. *Journal of Experimental Botany*, 1–10.

1150 **List of Tables**

1151	1	Values of the main parameters inherited from SUNFLO. . . .	52
1152	2	Sensitivity analysis of SUNLAB parameters: first-order in-	
1153		dices of the most influential parameters (with index > 1%). . .	53
1154	3	Estimated parameter values of SUNLAB for four genotypes. .	54

Table 1: Values of the main parameters inherited from SUNFLO.

Parameter	Parameter values			
Name	Albena	Melody	Heliasol	Prodisol
E1 ($^{\circ}\text{Cd}$)	510	540	480	510
F1 ($^{\circ}\text{Cd}$)	900	920	880	900
M0 ($^{\circ}\text{Cd}$)	1160	1160	1150	1120
M3 ($^{\circ}\text{Cd}$)	1800	2060	1940	1840
Nmax (#)	31	26	24	25
A1 (cm^2)	9999	9380	8707	8233
A2 (#)	18.9	15.4	15.3	15.9
A3 (cm^2)	488	613	670	498
k (#)	0.78	0.96	0.88	0.87

Table 2: Sensitivity analysis of SUNLAB parameters: first-order indices of the most influential parameters (with index $> 1\%$).

sinkA(cap)	sinkB(cap)	sinkA(intern)	SR(cap)	SR(intern)	sinkB(intern)	internEpdTT
0.51	0.12	0.12	0.05	0.03	0.02	0.02

Table 3: Estimated parameter values of SUNLAB for four genotypes.

Parameter Name	Param. values <small>(with associated standard error)</small>			
	Albena	Melody	Heliasol	Prodisol
sinkA(blade)	8.4 <small>(0.22)</small>	2.8 <small>(0.12)</small>	2 <small>(0.1)</small>	4 <small>(0.16)</small>
sinkA(petiole)	3.4 <small>(0.33)</small>	1.5 <small>(0.22)</small>	1.5 <small>(0.7)</small>	4.3 <small>(0.76)</small>
sinkA(internode)	2.2 <small>(0.12)</small>	3.5 <small>(0.05)</small>	2.2 <small>(0.07)</small>	3.8 <small>(0.08)</small>
sinkA(capitulum)	5.6 <small>(0.12)</small>	4.3 <small>(0.17)</small>	6.5 <small>(0.3)</small>	6.5 <small>(0.28)</small>
sinkB(blade)	14.8 <small>(0.4)</small>	2.3 <small>(0.16)</small>	2.1 <small>(0.18)</small>	3.6 <small>(0.26)</small>
sinkB(petiole)	16.8 <small>(1.8)</small>	4.1 <small>(6.4)</small>	2.7 <small>(0.76)</small>	4.2 <small>(0.5)</small>
sinkB(internode)	13.8 <small>(3.9)</small>	7.7 <small>(0.29)</small>	1.7 <small>(0.07)</small>	12.2 <small>(0.44)</small>
sinkB(capitulum)	3.4 <small>(0.22)</small>	2.5 <small>(0.23)</small>	6.1 <small>(0.44)</small>	5.8 <small>(0.52)</small>
SR(petiole)	0.5 <small>(0.04)</small>	0.2 <small>(0.03)</small>	0.24 <small>(0.03)</small>	0.43 <small>(0.04)</small>
SR(internode)	1 <small>(0.06)</small>	3 <small>(0.19)</small>	1.6 <small>(0.08)</small>	1.8 <small>(0.09)</small>
SR(capitulum)	1000 <small>(253)</small>	600 <small>(126)</small>	350 <small>(54)</small>	500 <small>(144)</small>

1155 **List of Figures**

1156 1 Water cycle processes as considered in the water budget mod-
1157 ule of SUNLAB 56

1158 2 Fraction of transpirable soil water $FTSW$ for three datasets
1159 “2001”, “2002a”, “2002b” 57

1160 3 Experimental data (dots) and simulation (lines) comparisons
1161 of blade dry mass, internode dry mass, and capitulum dry
1162 mass for the four genotypes - “Albena”, “Melody”, “Heliasol”,
1163 and “Prodisol” - in dataset “2001”. 58

1164 4 Sink strength variation based on SUNLAB estimated parameters 59

1165 5 Graphs A to D: experimental data (dots) and simulations
1166 (lines) comparisons for the “2001” (blue) and “2002a” (red)
1167 conditions of the radiation interception efficiency $RIE(d)$, to-
1168 tal blade area $AA(d)$, leaf number $N(d)$, cumulated dry above-
1169 ground biomass $CDM(d)$ and biomass compartments (capit-
1170 ulum, blades, petioles, internodes) for the “Melody” geno-
1171 type. Graph E: biomass compartments of “Prodisol” geno-
1172 type. Graph F: experimental data (dots) and simulations
1173 (lines) comparisons for individual blade biomass of “Helia-
1174 sol” genotype on different days in dataset “2001” (blue) and
1175 “2002a” (red). 60

1176 6 Model evaluation for genotype “Albena” using an additional
1177 experimental dataset: “2002b” (RMSE: 36.4; coefficient of de-
1178 termination: 0.95) 61

1179 7 Comparison of simulation and field data for individual blade
1180 area and biomass of genotype “Melody”; the right graph is the
1181 simulation of specific leaf area for the four genotypes 62

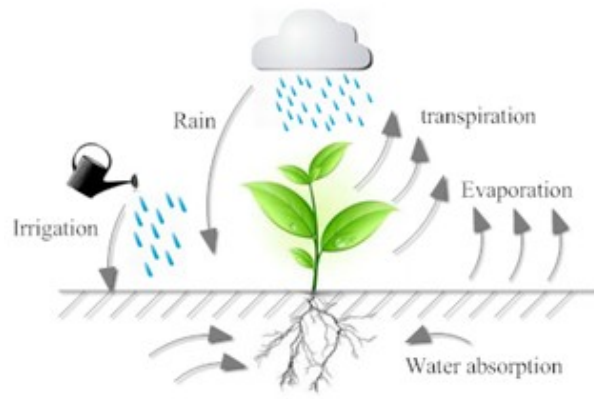


Figure 1: Water cycle processes as considered in the water budget module of SUNLAB

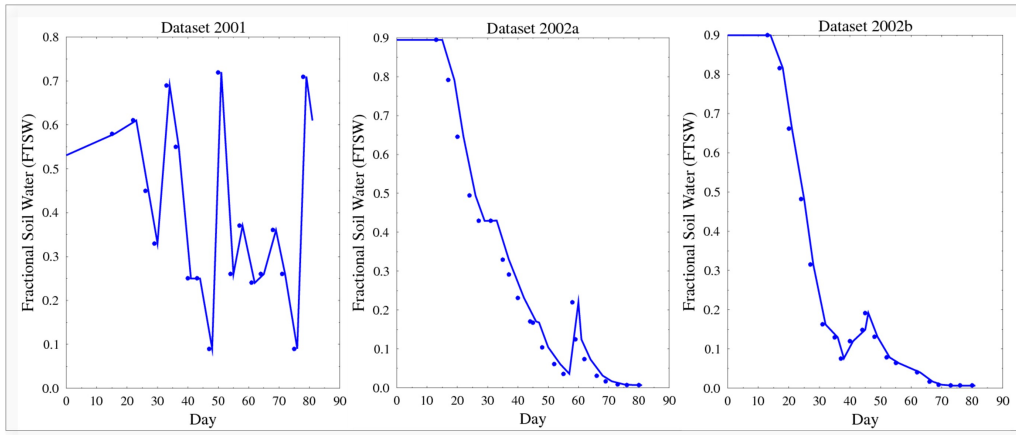


Figure 2: Fraction of transpirable soil water $FTSW$ for three datasets “2001”, “2002a”, “2002b”

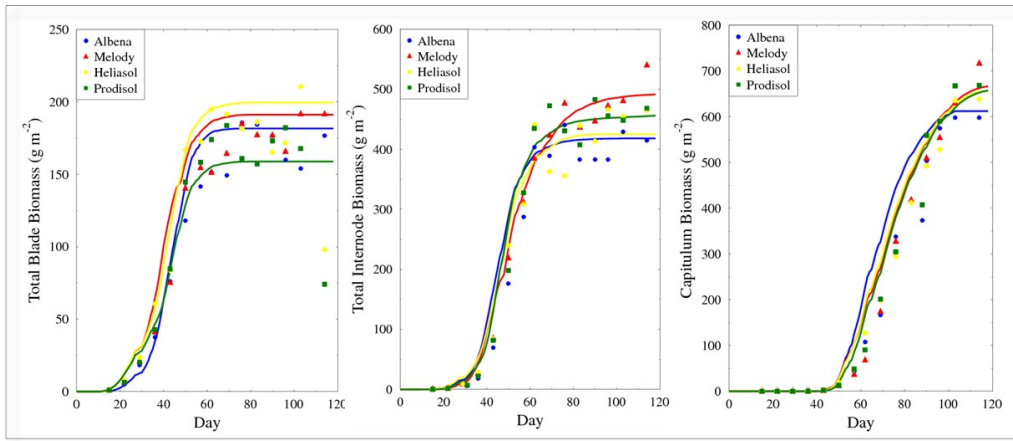


Figure 3: Experimental data (dots) and simulation (lines) comparisons of blade dry mass, internode dry mass, and capitulum dry mass for the four genotypes - “Albena”, “Melody”, “Heliasol”, and “Prodisol” - in dataset “2001”.

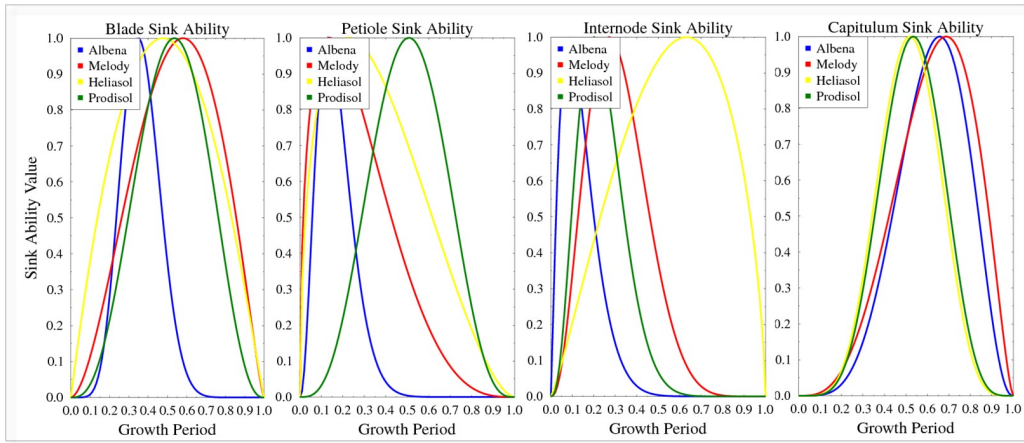


Figure 4: Sink strength variation based on SUNLAB estimated parameters

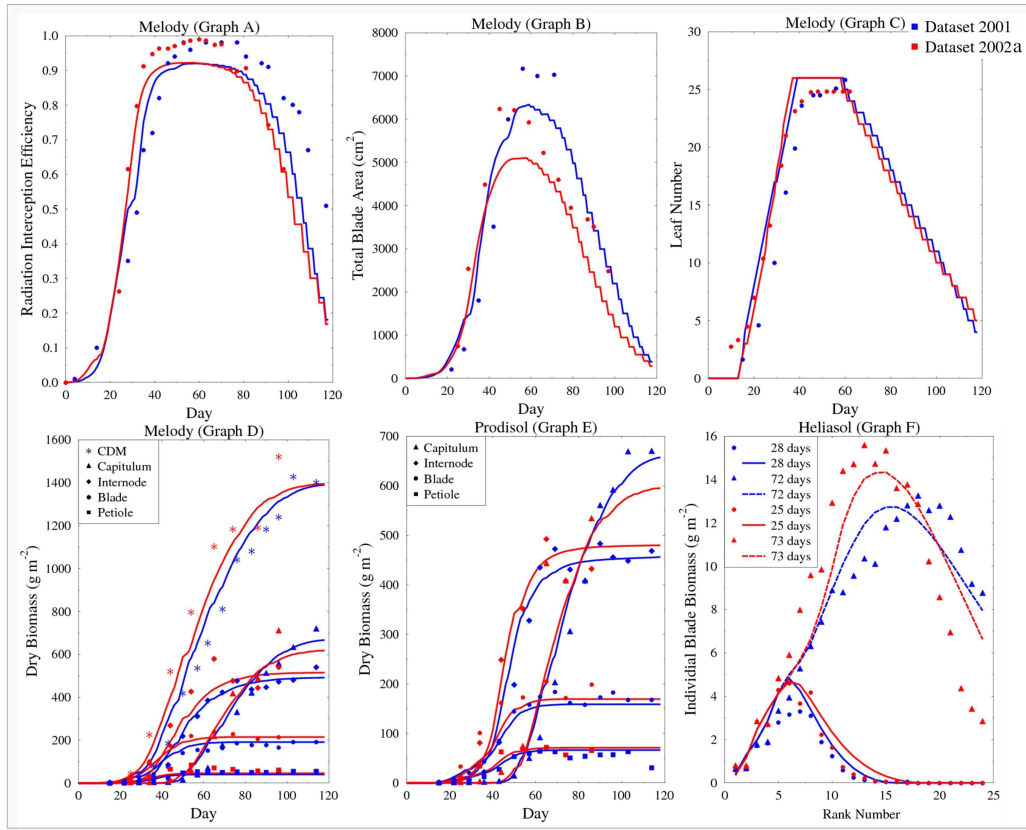


Figure 5: Graphs A to D: experimental data (dots) and simulations (lines) comparisons for the “2001” (blue) and “2002a” (red) conditions of the radiation interception efficiency $RIE(d)$, total blade area $AA(d)$, leaf number $N(d)$, cumulated dry above-ground biomass $CDM(d)$ and biomass compartments (capitulum, blades, petioles, internodes) for the “Melody” genotype. Graph E: biomass compartments of “Prodisol” genotype. Graph F: experimental data (dots) and simulations (lines) comparisons for individual blade biomass of “Heliasol” genotype on different days in dataset “2001” (blue) and “2002a” (red).

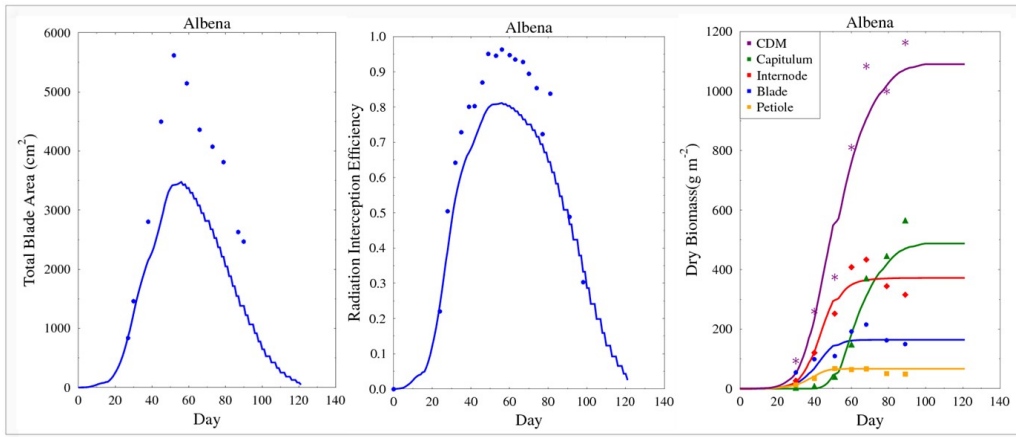


Figure 6: Model evaluation for genotype “Albena” using an additional experimental dataset: “2002b” (RMSE: 36.4; coefficient of determination: 0.95)

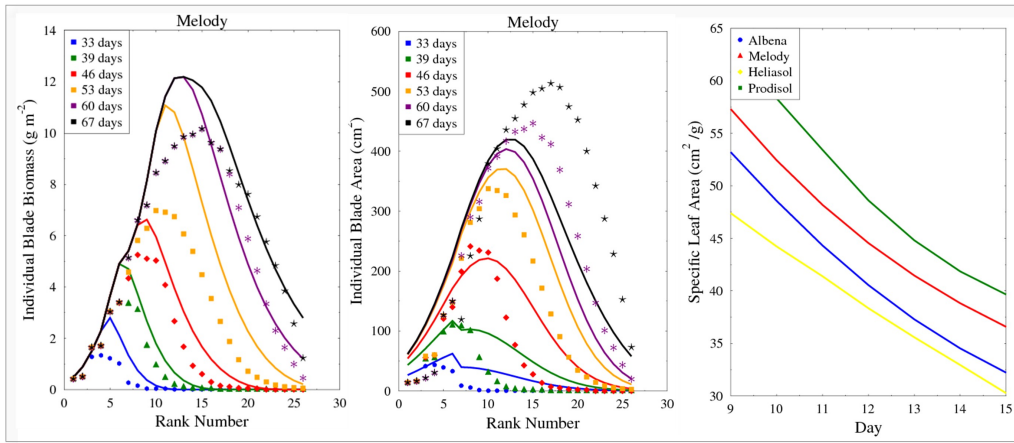


Figure 7: Comparison of simulation and field data for individual blade area and biomass of genotype “Melody”; the right graph is the simulation of specific leaf area for the four genotypes